Carbohydrate Research, 230 (1992) 201–212
Elsevier Science Publishers B.V., Amsterdam

The conformational behaviour of the cardiac glycoside digoxin as indicated by NMR spectroscopy and molecular dynamics calculations

Ann E. Aulabaugh [a], Ronald C. Crouch [a], Gary E. Martin [a], Aris Ragouzeos [a], John P. Shockcor [a], Timothy D. Spitzer [a], R. Duncan Farrant [b], Brian D. Hudson [b] and John C. Lindon [b]

[a] *Organic Chemistry Department, Burroughs Wellcome Co., 3300 Cornwallis Drive, Research Triangle Park, North Carolina 27709 (USA)*
[b] *Department of Physical Sciences, Wellcome Research Laboratories, Langley Court, Beckenham, Kent BR3 3BS (United Kingdom)*

(Received September 10th, 1991; accepted December 7th, 1991)

ABSTRACT

The ^{1}H- and ^{13}C-NMR spectra of digoxin in solution in Me_2SO-d_6 have been assigned completely. Measurement of the $^3J_{C,H}$ values has enabled estimation of the torsional angles involving the bonds linking the digitoxose residues, between the inner digitoxose and the genin unit, and for the unsaturated γ-lactone ring. These values have been supplemented by ^{1}H–^{1}H NOE data. In general, there is good agreement between the conformations in solution (NMR data) and the solid state (X-ray data), and that derived from theoretical modelling which shows evidence of conformational flexibility. The major difference occurs for the torsion between the genin and the innermost digitoxose residue where molecular dynamics predict the presence of two conformations, one similar to that seen by NMR and the other similar to the X-ray structure.

INTRODUCTION

Digoxin (digoxigenin-trisdigitoxoside, **1**) is an important drug extracted[1] from the leaves of *Digitalis lanata* and used in the treatment of heart arrhythmias. Even though the digitalis receptor is now associated with the enzyme Na/K-ATPase[2], the structure–activity relationships of cardiac glycosides remain complex[3,4]. Digoxin still remains a drug of choice despite its adverse therapeutic ratio and poor solubility. The structure–activity relationships in the area of cardiac glycosides are multi-faceted with changes to both steroid and glycoside parts of the molecule being involved in receptor recognition[3,4]. As a consequence, there is a need to

Correspondence to: Dr. J.C. Lindon, Department of Physical Sciences, Wellcome Research Laboratories, Langley Court, Beckenham, Kent BR3 3BS, United Kingdom.

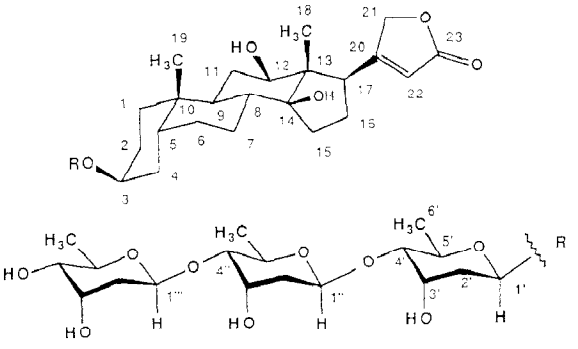

1

investigate the structure of such molecules, both in solution and in the solid state. Molecular structures of peptides are now calculated routinely using molecular dynamics methods[5], and digoxin represents a good test of their applicability to a non-peptide structure.

We now report the complete assignment of the ^{1}H- and ^{13}C-NMR spectra of digoxin (Table I), together with the $^{3}J_{C,H}$ values and ^{1}H–^{1}H NOE data. The molecular conformations of digoxin, calculated using molecular dynamics, have been compared to those in solution (NMR data) and in the solid state (X-ray crystal structure[6]), with the various inter-ring torsion angles τ_1–τ_7 defined in Table II.

EXPERIMENTAL

The ^{1}H-NMR spectra were measured for solutions in Me_2SO-d_6 at 25° with Bruker AM-360, Bruker AMX-500, and Varian VXR-500S spectrometers operating at 360.13, 500.13, and 499.84 MHz, respectively. Typically, 32K data points were used with a spectral width of 6300 Hz. Resolution enhancement of the free induction decay (FID) was by the Lorentzian–Gaussian method. Homonuclear 2D techniques involved COSY, TOCSY, and NOESY experiments. The COSY spectrum was acquired as 1K × 512 points (sine-bell weighting was applied in each dimension), zero-filled to 2K × 2K prior to FT, and symmetrised. The TOCSY spectrum was acquired as 2K × 512 points in a phase-sensitive manner[7], zero-filled to 2K × 2K points before FT, but not symmetrised. The NOESY spectrum was acquired as 1K × 256 points, again phase sensitive[4], with a mixing time of 700 ms and a 1.6-s interpulse delay, and zero-filled to 1K × 1K but not symmetrised. The ^{13}C-NMR spectra were acquired with Bruker AM-360 and Varian Unity 400 spectrometers operating at 90.54 and 100.58 MHz, respectively. As well as normal proton-decoupled spectra, fully coupled and DEPT spectra were acquired. Heteronuclear ^{1}H–^{13}C correlation spectra were acquired using the HMQC method[8], typically with an acquisition of 1K × 256 points zero-filled to 2K × 512 before FT.

TABLE I

Chemical shifts of the ^{1}H and ^{13}C resonances for digoxin

C-1	30.20	C-21	73.34	H-1α	1.28	HO-12	4.57
C-2	26.03	C-22	115.86	H-1β	1.34	HO-14	4.06
C-3	72.11	C-23	173.89	H-2α	1.48	H-1′	4.75
C-4	29.61	C-1′	95.34	H-2β	1.48	H-2′*eq*	1.73
C-5	36.34	C-2′	38.34	H-3	3.88	H-2′*ax*	1.53
C-6	26.46	C-3′	66.16	H-4α	1.69	H-3′	4.02
C-7	21.37	C-4′	81.70	H-4β	1.28	H-4′	3.12
C-8	40.49	C-5′	67.63	H-5	1.51	H-5′	3.66
C-9	31.63	C-6′	18.06	H-6α	1.14	CH_3'	1.07
C-10	34.69	C-1″	99.12	H-6β	1.71	HO-3′	4.15
C-11	29.73	C-2″	37.94	H-7α	1.06	H-1″	4.79
C-12	72.99	C-3″	66.30	H-7β	1.68	H-2″*eq*	1.83
C-13	55.72	C-4″	81.95	H-8	1.41	H-2″*ax*	1.58
C-14	84.29	C-5″	67.51	H-9	1.57	H-3″	4.04
C-15	32.45	C-6″	18.06	H-11α	1.41	H-4″	3.09
C-16	26.82	C-1‴	99.02	H-11β	1.05	H-5″	3.70
C-17	45.21	C-2‴	38.46	H-12	3.18	CH_3''	1.09
C-18	9.48	C-3‴	67.04	H-15α	1.82	HO-3″	4.21
C-19	23.70	C-4‴	72.70	H-15β	1.54	H-1‴	4.79
C-20	176.84	C-5‴	69.07	H-16α	1.95	H-2‴*eq*	1.83
		C-6‴	18.40	H-16β	1.80	H-2‴*ax*	1.56
				H-17	3.22	H-3‴	3.83
				CH_3(18)	0.63	H-4‴	2.98
				CH_3(19)	0.83	H-5‴	3.62
				H-21	4.89	CH_3'''	1.11
				H-21′	4.80	HO-3‴	4.59
				H-22	5.79	HO-4‴	4.57

TABLE II

Torsional angles (°) for digoxin and averaged interproton distances (Å) calculated from MD

Torsion definition	τ	NMR	X-ray	Mol. mechanics	Mol. dynamics [a]
H-17–C-17–C-20–C-22	1a	10	14	16	20 ± 30
H-17–C-17–C-20–C-21	1b	-170	-166	-166	-160 ± 30
H-3–C-3–O–C-1′	2	70	-45	15	35 ± 25 [b]
					-3 ± 20
H-1′–C-1′–O–C-3	3	50	21	57	60 ± 30 [c]
H-4′–C-4′–O–C-1″	4	~0	-50	-18	-10 ± 35
H-1″–C-1″–O–C-4′	5	30	38	57	50 ± 25
H-4″–C-4″–O–C-1‴	6	~0	5	-18	-15 ± 35
H-1‴–C-1‴–O–C-4″	7	30	60	58	55 ± 35

Atoms	Distance	Atoms	Distance
H-1′–H-1α	5.84	H-1′–H-3	2.57
H-1′–H-1β	4.71	H-1′–H-4α	4.13
H-1′–H-2α	4.66	H-1′–H-4β	3.06
H-1′–H-2β	4.06	H-1′–H-5	4.23

[a] The range of angles for a single conformation from MD. [b] Major conformation with a population of 60%. [c] A minor conformation at $-20° \pm 25°$ is also predicted.

Delays were optimised for an average value of 140 Hz for one-bond and 7 Hz for multiple-bond correlations using the HMBC sequence[9] at 500 MHz. In addition, SIMBA experiments[10] were performed with a selective Gaussian pulse to excite a single ^{13}C resonance. Assignments of some of the long-range $J_{C,H}$ values were confirmed by ^{13}C–{^1H} selective decoupling experiments.

Molecular dynamics (MD) simulations were performed on a Silicon Graphics IRIS 4D/320VGXB computer, using the program DISCOVER[11]. Partial charges were calculated[12] and held fixed during conformational changes. The dielectric constant was fixed at 1.0 and simulations were carried out without including any solvent molecules. During the dynamics simulations, the system was coupled[13] to a heat bath. The initial X-ray structure coordinates[6] were minimised in 648 iterations using the variable metric method, va09a, minimiser within DISCOVER with the CVFF force field. The simulations were initiated from the minimised coordinates at $-223°$ for 1 ps and were gradually warmed up to 27° in steps of 50° using 1-ps intervals. A period of 20 ps of equilibration was followed by 200 ps of simulation time at 27°. An integration time step of 1 fs was used throughout. Torsion angles (τ) were recorded every 50 fs. Additional calculations were performed at higher temperatures in order to investigate whether additional conformations would be populated. Some simulations were extended to 1 ns at 27° in order to investigate the possibility that conformational space was not being fully explored in a 200-ps dynamics calculation.

RESULTS

Assignment of the spectra.—The spectra were analysed in a sequential manner using the 1D and 2D experiments listed above. The γ-lactone ring was the starting point with H-22, since the resonance of the vinyl proton was identified easily and all proton and carbon signals for this ring were then assigned. The main steroid nucleus was assigned ring-by-ring starting with ring A at C-3/H-3. Thus, for example, the ^{13}C resonance at 72.11 ppm was shown by a DEPT experiment to be due to a CH moiety, which, from the HMQC result, was coupled to a ^1H resonance at δ 3.88, indicating a CHOH group. Additionally, a starting point in ring D at H-17/C-17 was used, the latter long-range coupled to H-22 in the COSY spectrum. Distinction from the various digitoxose resonances was achieved from the HMQC and TOCSY experiments which showed connectivities to *two* high-field resonances of methylene groups. Assignment of the sugar units started with H-1′ from the NOE observed from H-3. Stereochemical assignments of H-2′*eq*,2′*ax* was on the basis of NOE data and *J* values. The entry point for the assignment of the second digitoxose residue was through the NOE to H-1″ from H-4′, with the same procedure being used for the third digitoxose residue. The ^{13}C assignments are in agreement with literature data[14,15]. This work provides for the first time a complete assignment of the ^1H-NMR spectrum. The chemical shifts are summarised in Table I (from data at 500 MHz for ^1H, and 125 MHz for ^{13}C).

Inter-ring coupling constants.—Long-range $J_{H,C}$ values were measured from ^{13}C spectra, both fully and selectively ^{1}H-decoupled. The assignments were aided by the acquisition of a long-range $^{1}H-^{13}C$ 2D correlation spectrum. Thus, the torsion angle τ_{1a} (see Table II) is well defined because $J_{C\text{-}22,H\text{-}17}$ is clearly resolved as 5.4 Hz. Analysis of the resonance of C-21 shows two long-range couplings of 6.6 and 9.0 Hz. Since $^{3}J_{C,H}$ values involving *trans* sp^2 carbons have been found[16] to be in the range 9–10 Hz, the 9.0-Hz coupling is assigned to $J_{C\text{-}21,H\text{-}22}$ and the 6.6-Hz coupling to $J_{C\text{-}21,H\text{-}17}$. The definition of τ_2 was achieved by measuring $J_{C\text{-}1',H\text{-}3}$, but no correlation was seen in the 2D long-range correlation experiment, indicating a very small coupling. However, ^{1}H-decoupling at H-3 whilst observing C-1′ gave a value of 1.3 Hz derived from the reduction in the overall bandwidth on decoupling. Next, regarding the sugar torsion angles τ_3, τ_5, and τ_7, $J_{C\text{-}3,H\text{-}1'}$ was detected as a weak correlation in an experiment optimised for a 7-Hz coupling. The actual value was determined to be 4.0 Hz from a selective decoupling experiment by irradiating H-1′ and observing C-3. Both $J_{C\text{-}4',H\text{-}1''}$ and $J_{C\text{-}4'',H\text{-}1'''}$, which define τ_5 and τ_7, respectively, were measured as 4.5 Hz. On the other hand, τ_4 and τ_6 are defined by $J_{C\text{-}1'',H\text{-}4'}$ and $J_{C\text{-}1''',H\text{-}4''}$, respectively, each of which gave a strong correlation in the long-range 2D plot, indicating large values, probably > 5 Hz. Precise values could not be determined because of extensive overlap of the C-1″ and C-1‴ resonances.

Molecular dynamics simulations.—The various torsion angles are as defined in Table II, which also lists the relevant X-ray values and those calculated using molecular mechanics minimisation and molecular dynamics. During minimisation from the X-ray structure, a conformational change due to alterations in τ_2 and τ_3 occurred. The subsequent MD simulations at 27° did not deviate significantly from the minimised structure, so that the calculations predict essentially single values for all torsions except for τ_2 where there is evidence for exchange between two forms. As an example, Fig. 1 shows a plot of τ_2 and τ_3 over the 200-ps simulation. Thus, τ_1 and τ_4–τ_7 each show a single value, but τ_2 appears to flip between two conformations characterised by torsion angles of 35° and −30°. Analysis of the data indicates that the conformation with τ_2 35° is favoured with a population of ~ 60%. In addition, whereas τ_3 appears to have only a single *gauche* value (~ 60°) for most of the time, there are occasional excursions to a different conformation characterised by −20°. In addition, in higher-temperature simulations using MD, there is also evidence that the γ-lactone ring spends a minor portion of its time in the flipped conformation. Both τ_4 and τ_6 are predicted to be close to zero, and τ_5 and τ_7 are calculated to have values close to 60°, a *gauche* arrangement.

The torsion angles τ_5 and τ_7 are sometimes designated ϕ. Other experimental studies[17,18] have shown that ϕ usually has a value close to +60° when the glycoside linkage is β, as a result of the so-called exo-anomeric effect[19]. Thus, it appears that MD with the CVFF force field is reproducing this effect in a reasonable fashion. The value of τ_3, which is also of the ϕ type, was also calculated to be close to +60° as prediced from the exo-anomeric effect. The MD calculations

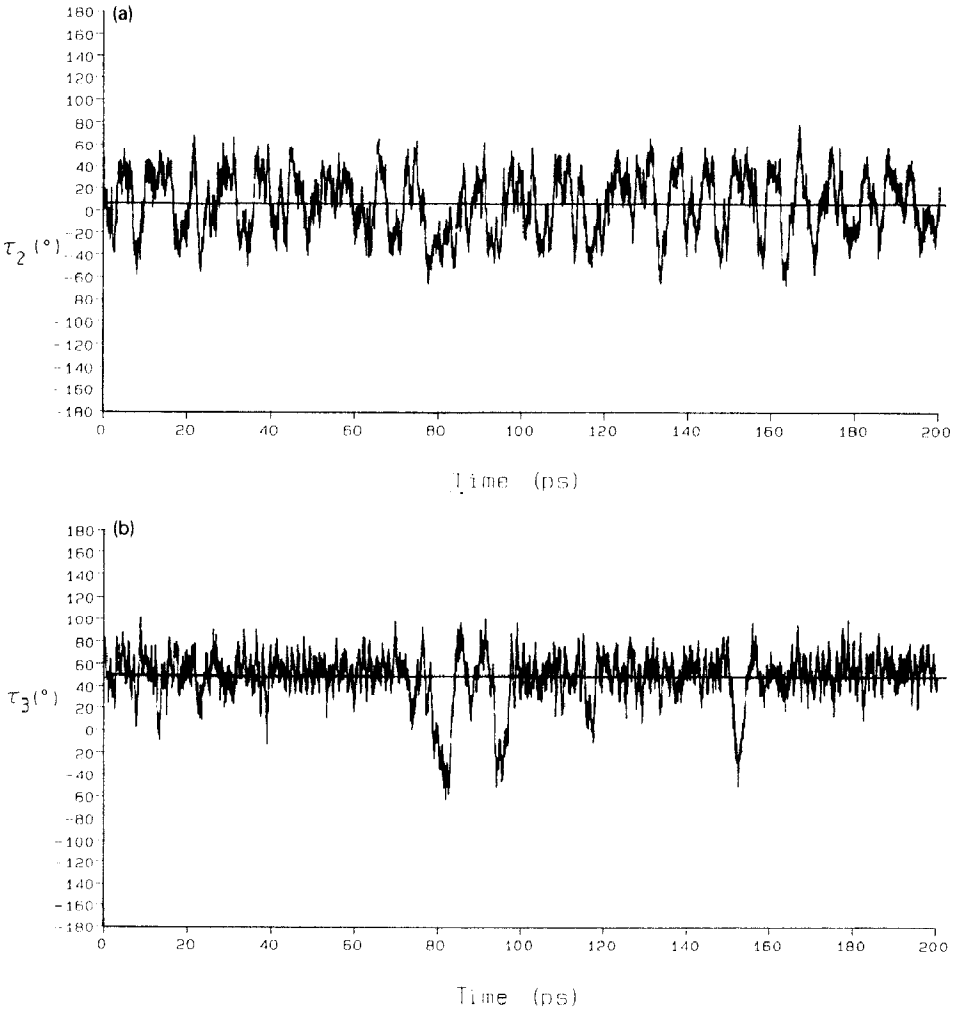

Fig. 1. Variation of τ_2 (H-3–C-3–O-1′–C-1′) and τ_3 (H-1′–C-1′–O-1′–C-3) with time as calculated by MD at 27°. The spread about the average values is shown as the error in Table II.

predict τ_4 and τ_6 to be near 0° and this angle is often designed by Ψ. This torsion angle is much less influenced by the exo-anomeric effect.

The values for ϕ and Ψ derived here can be compared with those from a recent MD study[20], using a specially modified AMBER[21] force field, in which a β-Man-(1 → 4)-GlcNAc linkage was calculated to have ϕ 51° and Ψ 0° in a simulation without inclusion of explicit solvent molecules but using a dielectric constant of 80 to approximate to the aqueous environment.

Table II also shows an estimate of the spread in torsion angle for each conformation at 27°. Based upon these simulations, it was possible to calculate various inter-proton distances in order to predict NOE values. In particular, Fig. 2

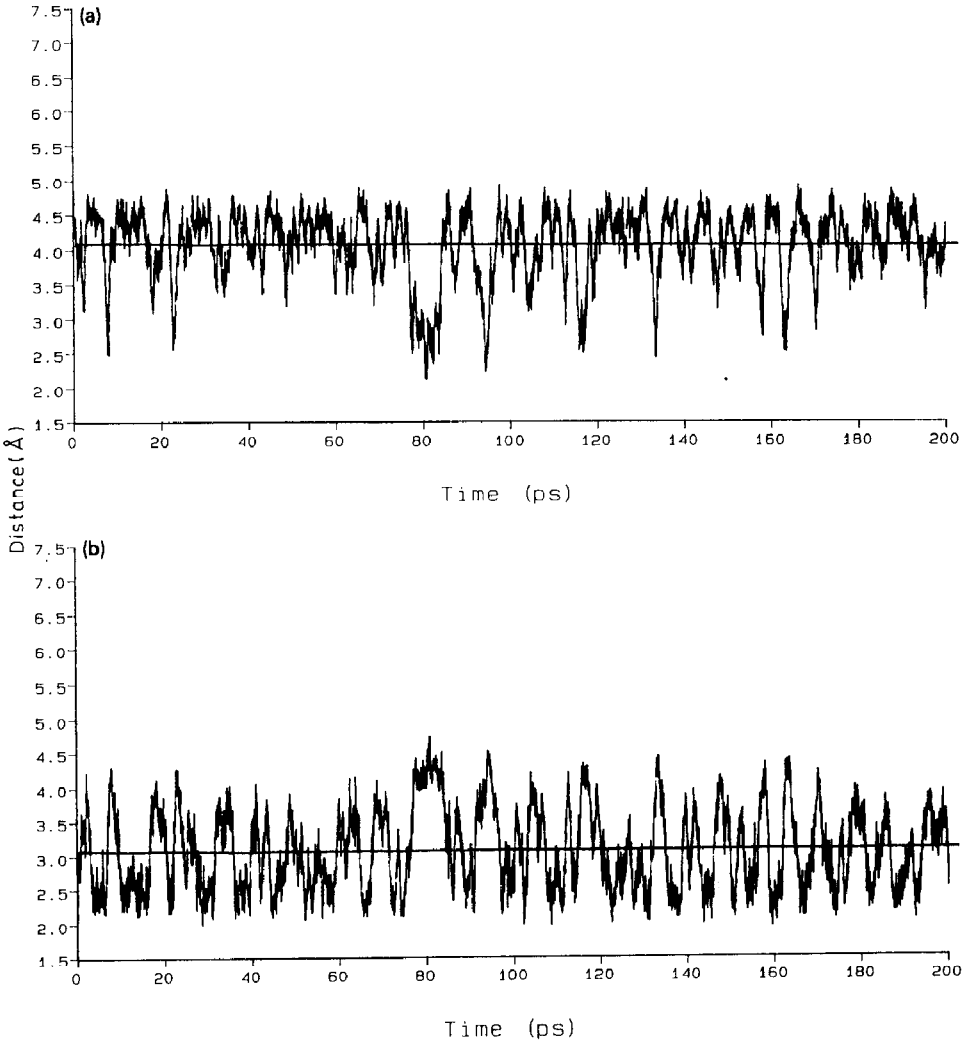

Fig. 2. Plot of the distances between (a) H-1′ and H-2β and (b) H-1′ and H-4β, as calculated as a function of time using MD at 27°, together with the mean value (———).

shows a plot of the H-1′–H-2β and H-1′–H-4β distances over the 200-ps simulation. MD calculation of distances between H-1′ and various hydrogens at 27° leads to the average values listed in Table II. Thus, NOEs are expected for H-3 and H-4β with potentially detectable responses for H-2β, H-4α, and H-5.

Simulations have also been extended to 1 ns in order to investigate whether the original calculations were sufficient to sample all the accessible conformations. These simulations showed that the 200-ps simulation gave a valid picture of the conformation for all of the torsion angles except for τ_3. The shorter simulations predicted a *gauche* conformation for τ_3 but, on extending the simulation to 1 ns, evidence was seen for the presence of the *trans* (180°) conformation, which was present for ~ 4% of that period.

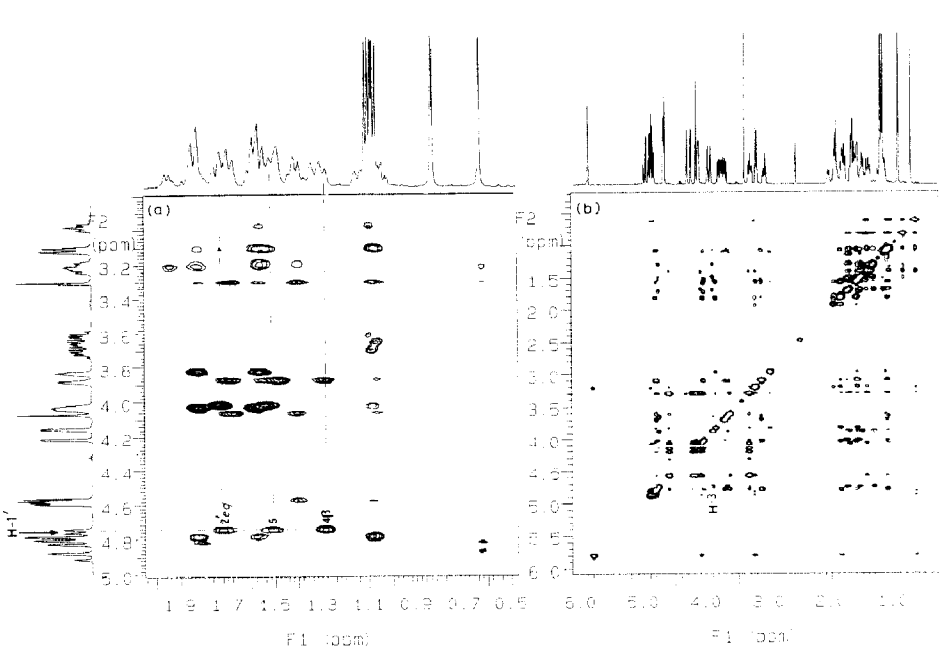

Fig. 3. ^{1}H–^{1}H NOESY spectrum of digoxin at 500 MHz, showing interactions of H-1′ and H-2′*eq*, H-3, H-4β, and H-5: (a) expanded region; (b) full spectrum.

^{1}H–^{1}H NOE connectivities.—2D ^{1}H–^{1}H NOESY observations served to confirm the general conformational picture. Fig. 3 illustrates that NOEs are observed from H-1′ to H-3, H-4β, and H-5, but not to H-1β. It was not possible to observe whether an NOE existed from H-1′ to H-1α but, in all reasonable conformations, these two nuclei are at such a distance as to make this impossible. In addition, it was not possible to observe NOEs from H-1′ to the coincident resonances of H-2α and H-2β, because of peak overlap with that of H-5. Thus, the available data indicate that τ_2 and τ_3 have values consistent with those in Table II, such that the average value for the first digitoxose residue is twisted to place H-1′ closer to the H-4/H-5 part of the genin A ring (see Fig. 4). Next, NOE's are observed from H-1″ to H-4′ and Me-6′, indicating that τ_4 and τ_5 have values such that the second digitoxose is twisted to one side, consistent with the values of τ_4 0° and τ_5 30° given in Table II. The orientation of the third digitoxose residue, both from NOEs and *J* values, is similar to that of the middle sugar. NOEs are seen from H-22 to H-17 and weakly to HO-14, H-16β, and Me-18, showing that the γ-lactone ring resides in the conformation with H-22 mainly on the α face but also spending a smaller proportion of time in an inverted conformation.

Comparison of torsion angles derived from the three techniques.—The various torsion angles have been calculated from the $^3J_{C,H}$ values, using an equation parameterised for carbohydrates[22], and these are listed in Table II. Because of the nature of the equation, it is not possible to distinguish torsion angles symmetrically disposed around 0° and 180°. In some instances, distinction is made on the basis of

the NOE measurements; otherwise, the NMR-derived values are of undefined sign.

The γ-lactone torsion is well defined with two independent NMR observations: τ_{1a}, derived from $J_{C\text{-}22,H\text{-}17}$, has a value of 10°, and τ_{1b}, derived from $J_{C\text{-}21,H\text{-}17}$, has a value of 170°. It is likely that one of these values is negative because, by definition, they should differ by 180°. The X-ray structure has a value of 14° for τ_{1a} and the MD average value is ~20° at 27°. Repeating the MD at a higher temperature leads to a similar average value, but with occasional ring flips to a conformation characterised by a τ_{1a} changed by 180°. Thus, there is good agreement between all techniques for this torsion.

The torsion angles defining the conformation of the genin in relation to the first digitoxose ring are τ_2 and τ_3, and the J data indicate values of 70° and ~50°, respectively. From NOE evidence (see preceding section), a value of +70° is preferred for τ_2, which places H-1′ in proximity to H-4 and H-5. The corresponding X-ray values are −45° and 21°. The MD calculations predict two conformations for τ_2, of which the minor one is quite close to the X-ray structure. The other is similar to the NMR structure with a positive *gauche*-like value for τ_2. The presence of the major conformation is inferred by NOE measurements and the minor conformation cannot be ruled out because the detection of diagnostic NOE's was hampered by extensive peak overlap. For τ_3, there is good agreement between the MD and NMR results, each of which indicated conformations that are more twisted than the X-ray structure, with the NMR value and the calculation both in agreement with the empirical prediction based on the exo-anomeric effect.

The inter-glycosidic torsion angles τ_4 and τ_5 are calculated to be 0° and 30°, respectively, from the NMR data (cf. −50° and 38° from the X-ray data). Hence, the NMR data suggest a more eclipsed conformation than in the solid state, and this is supported by the MD which yields values of −10° and 50°, respectively. Again, there is reasonable agreement between the conformations indicated by NMR spectroscopy and MD and that predicted from the exo-anomeric effect, but each differs from the X-ray structure. For the torsion angles involving the third sugar unit, there is reasonable agreement between all three techniques for τ_6 in that NMR gives a value of 0°, the X-ray value is 5°, and the MD prediction is −15°. For τ_7, the agreement is not so good; the X-ray and MD results are comparable and agree with the exo-anomeric effect, but are somewhat larger than the NMR result. All the values are summarised in Table II, and representations of the structures derived from the various techniques are shown in Fig. 4.

Thus, although the NMR results reflect the average of a complex dynamic equilibrium, there are significant differences between the solution conformation and the solid-state structure as determined by X-ray crystallography. The principal difference involves the torsion angles of the glycosidic bonds between the genin and the innermost digitoxose residue. Molecular dynamics simulations of 200 ps are not sufficient to probe completely the accessible conformations for digoxin and probably these need to be extended by at least a factor of five. The molecular

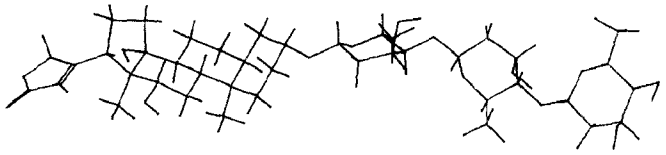

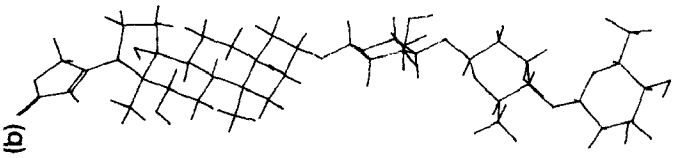
(b)

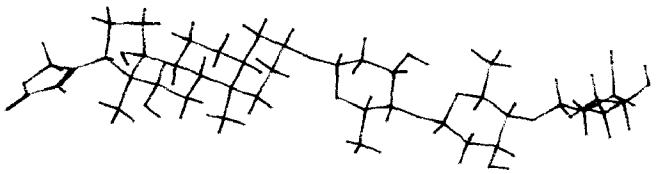

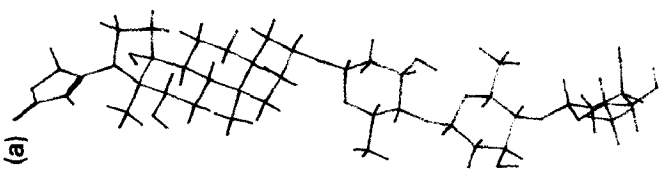
(a)

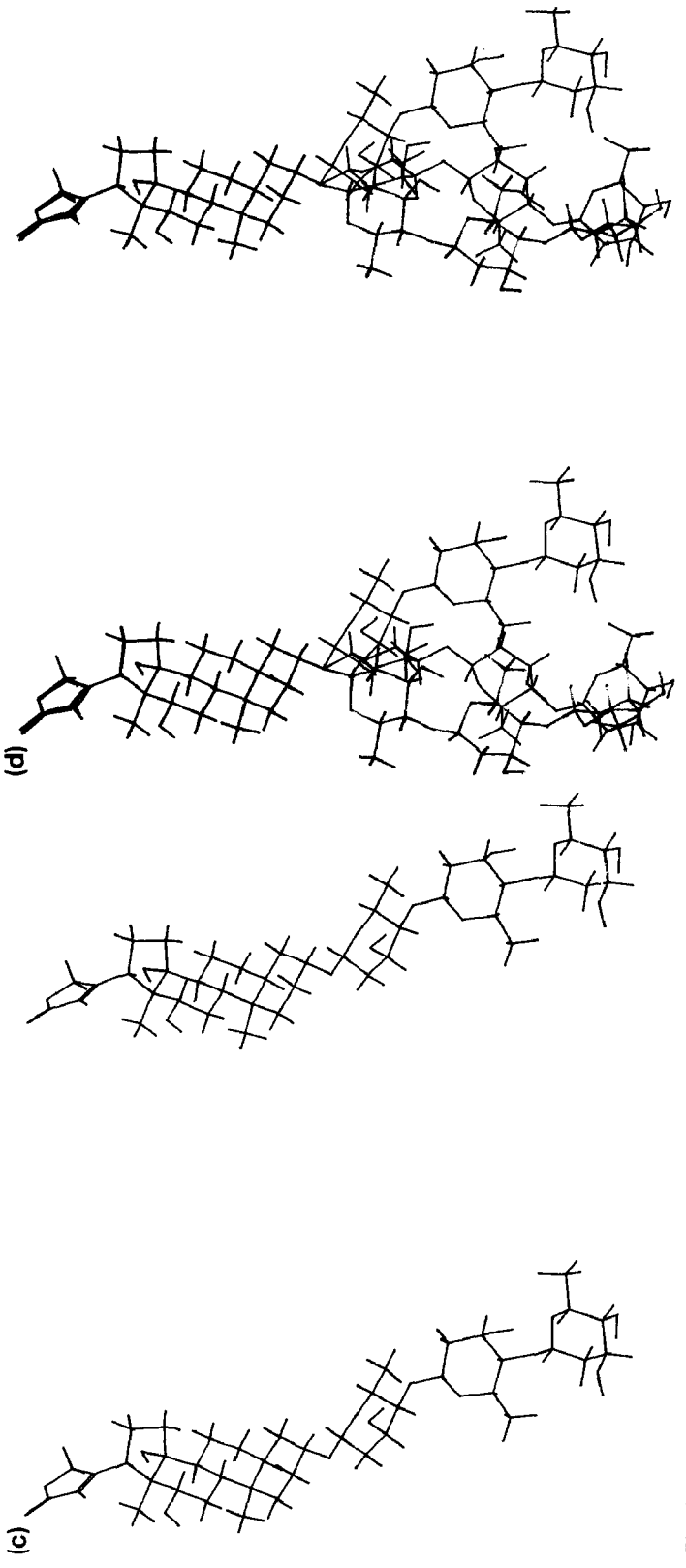

Fig. 4. Stereo-pair diagram of the conformation of digoxin as found by (a) X-ray crystallography, (b) MD, (c) NMR spectroscopy, and (d) a superposition of all three structures.

dynamics calculation in vacuo shows evidence of conformational flexibility which, in general, is closer to the solution conformations than those in the solid state.

In general, therefore, the unconstrained molecular dynamics calculation reasonably reproduces the solution-state NMR observations despite not being parameterised specifically for carbohydrates and without the explicit inclusion of solute–solvent force field parameters.

ACKNOWLEDGMENTS

We thank Dr. J.A.B. Lohman (Bruker Spectrospin, Coventry) for measuring some of the ^{1}H-NMR spectra at 500 MHz, especially the long-range ^{1}H–^{13}C correlation, and M. Watkinson for assistance with the MD calculations.

REFERENCES

1 S. Smith, *J. Chem. Soc.*, (1930) 508–510.
2 K.R.H. Repke and W. Schonfeld, *Trends Pharmacol. Sci.*, 5 (1984) 393–397.
3 H. Rathore, A.H. From, K. Ahmed, and D.S. Fullerton, *J. Med. Chem.*, 29 (1986) 1945–1952.
4 W. Schonfeld, R. Schonfeld, K.H. Menke, J. Weiland, and K.P. Repke, *Biochem. Pharmacol.*, 35 (1986) 3221–3231.
5 J.A. McCammon and S.C. Harvey, *Dynamics of Proteins and Nucleic Acids*, Cambridge University Press, 1987.
6 K. Go, G. Kartha, and J.P. Chen, *Acta Crystallogr., Sect. B*, 36 (1980) 1811–1819.
7 D.J. States, R.A. Haberkorn, and D.J. Ruben, *J. Magn. Reson.*, 48 (1982) 286–292.
8 A. Bax and S. Subramanian, *J. Magn. Reson.*, 67 (1986) 565–569.
9 A. Bax and M.F. Summers, *J. Am. Chem. Soc.*, 108 (1986) 2093–2094.
10 R. Crouch and G.E. Martin, *J. Magn. Reson.*, 92 (1991) 189–194.
11 Biosym Technologies Inc., San Diego, CA, U.S.A.
12 J. Gasteiger and M. Marsili, *Tetrahedron*, 36 (1980) 3219–3228.
13 H.J.C. Berendsen, J.P.M. Postma, W.F. van Gunsteren, A.D. Nola, and J.R. Haak, *J. Chem. Phys.*, 81 (1984) 3684–3690.
14 L. Brown, H.T.A. Cheung, R. Thomas, T.R. Watson, and J.L.E. Nemorin, *J. Chem. Soc., Perkin Trans. 1*, (1981) 1779–1781.
15 W. Robien, B. Kopp, D. Schabl, and H. Schwarz, *Prog. Nucl. Magn. Reson. Spectrosc.*, 19 (1987) 131–181.
16 P.E. Hansen, *Prog. Nucl. Magn. Reson. Spectrosc.*, 14 (1981) 175–296.
17 R.U. Lemieux, K. Bock, L.T. Delbaere, S. Koto, and V.S. Rao, *Can. J. Chem.*, 58 (1980) 631–653.
18 H. Thorgersen, R.U. Lemieux, K. Bock, and B. Meyer, *Can. J. Chem.*, 60 (1982) 44–57.
19 I. Tvaroska and T. Bleha, *Adv. Carbohydr. Chem. Biochem.*, 47 (1989) 45–123.
20 S.W. Homans, *Biochemistry*, 29 (1990) 9110–9118.
21 S.J. Wiener, P.A. Kollman, D.T. Nyugen, and D.A. Case, *J. Comput. Chem.*, 7 (1986) 230–252.
22 C. Morat and F.R. Taravel, *Tetrahedron Lett.*, 31 (1990) 1413–1416.